Technical Journal, University of Engineering and Technology (UET) Taxila, Pakistan Vol. 23 No. 3-2018
ISSN:1813-1786 (Print) 2313-7770 (Online)

Lubrication Analysis of Piston Secondary Motion using Gauss Seidel Iterative Technique

R. Kalvin[1], A. Nadeem[2], A. Tariq[3], B. Nadeem[4]

[1,3]Mechanical Engineering Department, Wah Engineering College, University of Wah, Pakistan
[2]Inha University, South Korea
[4]Mechanical Engineering Department, University of Engineering and Technology Taxila, Pakistan
[1]Roman.kalvin@wecuw.edu.pk

Abstract-This research deals with the analysis of lubrication exaggerated by the secondary motion of the piston. The quality of lubrication is affected by oil consumption, fuel efficiency and emission of exhaust gases. Therefore this technique is used to make a mathematical model of piston. It is further analyzed on MATLAB using Gauss Seidel iterative method to get the required results and see the effects on lubrication layer caused by piston tilt motion. The technique used in this research is by discretizing the equations and making matrices of the required forces for different crank angles. Also mesh is being generated at piston skirt. Across each node of mesh the effect of lubrication layer was observed. The results extracted from the research showed that the lubrication regimes changes and affect piston secondary motion and hydrodynamic film thickness is maximum at the top of the skirt but as piston moves from top dead center to bottom dead center, it decreases on the lower edge of the skirt and hydrodynamic pressure also acts on the skirt on thrust side of the cylinder.

Keywords-MATLAB, Lubrication, Gauss Seidel Iterative, Crank Angles

I. INTRODUCTION

In piston cylinder assembly of the engine, piston does not move only in the reciprocating direction but it executes its motion in lateral direction also. This movement of the piston in the lateral path is called piston secondary motion. As there is narrow clearance among the piston skirt and cylinder liner so, there must be the very small movement of the piston in lateral direction. But the performance of the engine is significantly pretentious by the secondary movement of the piston, situations of lubrication is determined by the secondary motion of the piston. As secondary motion affects the piston lubrication so at the meeting point of piston ring-cylinder liner friction is generated due to which about 20-25% mechanical efficiency loss is caused. Furthermore, oil consumption, fuel economy, durability, exhaust emissions, and noise emission are greatly affected by the quality of lubrication. Fig. 1 represents power consumption obtained from an engine of medium sized vehicle [I].

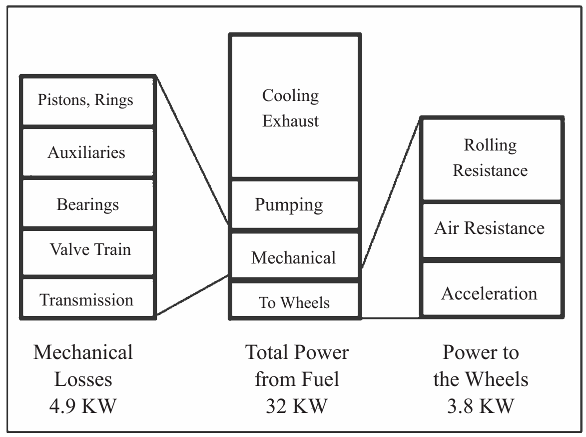

Fig. 1. Consumption of power obtained from an engine of medium sized passenger vehicle

At high crank speed lubrication layer cannot cushion the lateral movement of the piston and piston hits the cylinder liner causing piston slap which affects the efficiency of the engine and noise is produced. When speed of piston lateral motion becomes greater than specific values it goes towards the cylinder wall, film thickness fails to provide support to the piston skirt. A few design factors such as crank offset, piston pin offset, lubricated surfaces excellence and lubricant traits are really helpful for the ease of piston operation during secondary movement. Viscosity of the lubricant defines its frictional and damping action. Viscosity is beneficial in evading the friction; on the other hand load carrying ability of the lubricant is declined. Earlier studies of piston considered the piston to be stiff and lubrication was not taken into account.

II. LITERATURE REVIEW

Than as further studies and research was done lubrication effects and elastic deformation was taken into account. The authors of [ii] studied and established the asperity contacts between the two faces. Mostly between two sliding surfaces only one was considered rough and other was smooth. They also took into account the elastic deformation of the two sliding surfaces asperities. The authors of [iii] studied Reynolds equation by adding 3D coarseness on hydrodynamics lubrication film. They also considered the combined roughness factors of both surfaces into equation. And to find the effect of direction of surface and how it affects lubrication film as also considered. A model of skirt lubrication was created by [iv] investigated piston secondary dynamics examination lubrication with taking surface coarseness into account by using Reynolds equation. Elastic deformation was taken as input. In order to take oil unavailability, lubrication level was also considered as an input and Reynolds equation was improved accordingly. Then this model was integrated with piston's secondary dynamics defined by [v],they studied wrist pin hydrodynamic and lubrication within its bearing. To decrease the processing period the hydrodynamics and contact pressures were carried out in separate coded and then integrated with secondary dynamics model.

The objectives of [vi] was studied piston secondary movement and piston smack due to lateral motion in incompletely flooded elasto-hydrodynamic lubrication, by using improved Reynolds equation .Negative clearance values were present as piston diameter were considered larger than the bore diameter and prevented by setting very small clearance value at every grid point at initialization of iteration until the nonnegative values are achieved. To determine the secondary motion of piston.[vii] developed an original simulation program for reciprocating engine with elastic deformity. This includes equations of motions using single degree of freedom with varying speed of crank. A general code was generated to solve equations of motion using any number of cylinders as required. And friction was by using Stribeck diagram.

The authors of [viii] enhanced the design of non-cylindrical, ring-less piston which was lubricated by gas. For pressure distribution calculations they used non dimensionalized Reynolds equation neglecting flow factors. They provided optimized results considering piston stability and leakage of gas.[ix] studied ring-less pistons of reciprocating compressors. Technique was using simplified Reynolds equations and neglecting surface roughness. Assumptions were that piston and cylinder liner is rigid and hydrodynamic lubrication is used. This test seems to be valid for complete engine cycles.[x] developed an explanatory model of piston's secondary motion taking account of hydrodynamic lubrication, asperity contact and surface coarseness. Elastic deformation is only considered in asperity contact condition. Broyden solution was only one that converges than other methods. Other tests were also made like laser induced fluorescent method, micro-focusing system, input fiber, fiber bundle receiving probe.[xi] developed algorithm for hydrodynamic lubrication, inclusive of coarseness pressure due to contact and cavitation. No assessment of secondary dynamics was observed. Only this model was integrated with FE model for piston-liner. And results were validated with previous methods and evaluated. [xii] improved the model design of half flooded lubrication case and cavitation factor. To check the limit of lubrication Reynolds equation for journal bearing code, ORBIT was utilized for piston skirt and cylinder liner assembly lubrication. Nodal analysis was done to check and differentiate between flooded and cavitation nodes. Mass terms in two dimensional Reynolds equation were used in discretized form. The specification of oil supplied allowance is measured by cavitation region being represented more accurately.[xiii] studied the effect of fire causing wear on ring. Reynolds equation for unidirectional flow without roughness effect are being solved. They calculated the hydrodynamic frictional force and boundary lubrication friction from Stribeck diagram. Pistons secondary motion and lubricant cavitation wasn't considered.[xiv] solved using contact feature and simple Reynolds equation for less measureable time by using single directional flow.[xv] solved for piston's ring lubrication system. Using boundary conditions defined by JFO for cavitation. Also introduced open and closed cavitation patterns. Conditions were applied at points where reformation is in bounded cavitation.[xvi] developed a simple system for piston rings friction use Reynolds equation and Stribeck curves to calculate friction including geometry of system and roughness. The authors of [xvii] resolved by using one direction Reynolds equation as in the system of [xiv] inclusive of cavitation procedure. Film rupture was also observed and analyzed by Reynolds (Swift-10 Stieber) boundary conditions considering surface coarseness and asperity contact.[xviii] investigated the consequence of lubricant viscosity on the temperature and thickness of oil film on a piston ring in a diesel engine by using unsteady state thermo hydrodynamic lubrication analysis.[xix] evaluated the tribological behavior of nano-lubricants using a tribometer under different operating conditions to imitate the liner interface. The outcome showed the decrease in friction coefficient and power losses. The objectives of [xx] used laser induced fluorescence system to a piston ring ,cylinder bore friction and reciprocating liner configuration of the test bench system allows the collection of continuous lubricant film thickness data at different crank angle position.[xxi] enhanced the viscosity-grade of an engine lubricant to reduce the adhesive wear of the piston skirts and cylinder liner when engine startup.[xxii] reviewed the fundamentals of friction specific to the environments of engine components tribology as well as effect of friction due to lubricant. [i] studied cavitation effect in rings by giving comprehensive analysis of borderline conditions discussed in rupture and reformation of film. By applying these conditions results were obtained and compared. When two rough sliding surfaces are in contact with each other then three different behaviors of lubrication can be observed. Which are as:

- Mixed lubrication
- Hydrodynamic lubrication
- Elasto-hydrodynamic lubrication
- Boundary lubrication

There is an asperity contact of both the sliding surfaces to some level in mixed lubrication regime. Between the sliding surfaces fluid film is formed but this film is continuously deformed due to the asperities of the surfaces passing through. Both hydrodynamic and boundary lubrication characteristics can be observed in mixed lubrication regime. Surfaces are completely separated in hydrodynamic lubrication regime. In regards of surface separation, both elasto-hydrodynamic lubrication and hydrodynamic lubrication are alike, but as a result, the effect of elastic deformations is more significant because small clearance between the surfaces or the surface contact has to bear a high normal load. Furthermore, viscosity depending on pressure is of high importance in this regime. Dynamic viscosity is the most important property of the lubricant. In boundary lubrication regime surfaces are in too much vicinity to each other so a good lubrication layer cannot be formed between the surfaces. The effect of lubricant between the surfaces is very less. H_σ= 3 acts as the point of transformation from mixed lubrication regime to hydrodynamic lubrication regime. If H_σ<3 then the lubrication is termed as partial lubrication. As the surfaces get apart from each other, the number of asperity peaks interacts with the asperities of the other surface and in result of that asperity peaks worn out and regime shifts towards hydrodynamic lubricant regime.

In boundary lubrication regime friction coefficient remains approximately constant. Friction coefficient remains resistant to the change in relative velocity, normal contact load or lubricant viscosity. In start of the process as the film thickness increases friction coefficient values does not change up to a specific value of lubricant thickness but as the layer of lubricant becomes thicker than the specific value, fluid film becomes effective in load handling. As the lubrication regime changes to mixed lubrication regime, coefficient of friction starts decreasing, because of the higher lubrication layer than in boundary lubrication regime. It lowers till the asperity contact becomes minor, and due to the insignificant asperity contact full lubrication layer is established between the sliding surfaces and hydrodynamic lubrication regime is achieved. So, for a steady-state elastohydrodynamic contact application that is not changing with time, operation in the section where lubrication regime changes from mixed to hydrodynamic lubrication is carried out to minimize friction loss. Sommerfeld group shifts slightly towards hydrodynamic region in order to reduce surface contact and reduce wear of the material. As piston operates in transition region the high asperity peaks of rough surfaces are worn out and lubrication shifts towards hydrodynamic lubrication.

Though, steady-state operation is impossible in internal combustion engine or in lubrication of compressor piston assembly, because of the variable forces of hydrodynamics and friction applying on the piston skirt throughout a whole power stroke, even at unvarying speed and load conditions. Fig. 3-2, depicts the properties of lubrication with few more engine lubricated parts. Lubrication regions, both Mixed and hydrodynamic, are used in Piston ring and skirt lubrication.

Quality of lubrication in sliding surfaces greatly depends upon the amount of lubricant supplied to the elasto-hydrodynamic contact. To form a film layer greater quantity of lubrication has to present at its leading edge in hydrodynamic contact. With the decrement of this amount of lubricant, lubrication regime shifts towards the boundary lubrication regime.

The lubrication thickness on the walls of the cylinder at the leading edge side represents the amount of oil supply. Due to the convergent section of barrel profile, as the supply oil film thickness increases leading edge side acts as an inlet location and length of lubrication supporting load increases, as in Fig. 3-3. For an internal combustion engine piston skirt, oil ring sets this lubrication thickness as piston moves towards top dead center, and by the amount of oil remained from the foregoing power stroke of piston and lubricating process for instance oil jet and splashing of crank as the piston moves towards bottom dead center. In the case of the ringless compressor piston movement towards top dead center, oil supply is inadequate by only the residual amount from the down stroke. So oil supply mechanism design has vital importance in this study.

Depending on the amount of oil at the start of the process, inlet conditions are differentiated as:

- Starved inlet
- Partially-flooded inlet
- Fully flooded inlet

Adequacy of oil is determined by linking the present thickness of oil to the design estimated value of the oil.

In major lubrication studies, stationary inlet location is set and fully-flooded lubrication at inlet condition is considered. Accurate inlet location can be estimated using the piston alignment at some instant and structural relations of barrel profile to calculate the thickness of oil supply. Rough predictions may be more practical because proper calculations for the supply oil thickness can be too much complex.

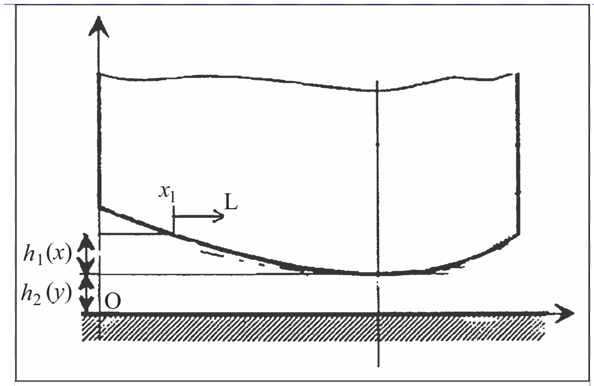

Fig. 2. Effect of thickness of supply oil on functional lubricated length

Effective length of lubricant film does not remain effective at the outlet location and loses its capacity to carry load and does not stick to the sliding surface. When outlet location is nearer to the trailing edge then that design is considered as effective design. This in turns increases the effective lubrication length and its load carrying capacity increases and smoother operation is providing to the piston. In accordance with the possible farthest outlet and inlet locations, piston skirt length is determined in piston skirt lubrication. Due to the barrel profile of the skirt it may be possible that some surface at the leading or trailing edge remain un-wetted at any operational conditions, the un-wetted section either is cut out to minimize mass of the piston or barrel shape is straighten to use the complete length of skirt.

Trailing edge pressure was set as outlet pressure [xxii].

At $x = x_1$, $p = p_L$

At $x = x_4$, $p = p_T$

A. Governing Equations

1) Reynolds Equation

Pressure is controlled by Reynolds equation in the lubricant in Elastohydrodynamic contacts whose viscosity is not affected by the change in temperature:

$$\frac{\partial}{\partial x}\left(\frac{h_T^{\,3}}{12\mu}\frac{\partial p}{\partial x}\right)+\frac{\partial}{\partial y}\left(\frac{h_T^{\,3}}{12\mu}\frac{\partial p}{\partial y}\right)=\frac{U_1+U_2}{2}\frac{\partial h_T}{\partial x}+\frac{\partial h_T}{\partial t} \quad (1)$$

h_T is mean local thickness, U_1 and U_2 are absolute velocities of sliding surfaces and x being the sliding direction.

In equation (1), the last term on the right hand side is the squeeze film velocity and the first term is the mass transport due to change in the film thickness in the direction of the flow of lubricant. The two terms on the left hand side are the mass transport in x and y-directions, respectively, due to pressure gradient. As the surfaces move toward or away from each other the change in the lubrication film thickness happens. This effect is called squeeze film effect.

To incorporate effects of surface roughness, Reynolds equation was modified by [ii] which is as follows

$$\frac{\partial}{\partial x}\left(\frac{h_T^3}{12\mu}\frac{\partial\bar{p}}{\partial x}\right)+\frac{\partial}{\partial y}\left(\frac{h_T^3}{12\mu}\frac{\partial\bar{p}}{\partial y}\right)=\frac{U_1+U_2}{2}\frac{\partial\bar{h}_T}{\partial x}+\frac{U_1-U_2}{2}\sigma+\frac{\partial\bar{h}_T}{\partial t} \quad (2)$$

One of the surfaces, in piston skirt-cylinder bore interaction, is stationary, $U_1 = U$ and $U_2 = 0$.
So eq. (2) is written as:

$$\frac{\partial}{\partial x}\left(h^3\frac{\partial\bar{p}}{\partial x}\right)+\frac{\partial}{\partial y}\left(h^3\frac{\partial\bar{p}}{\partial y}\right)=6\mu U\left(\frac{\partial\bar{h}_T}{\partial x}+\sigma\frac{\partial\phi_s}{\partial x}\right)+12\mu\frac{\partial\bar{h}_T}{\partial t} \quad (3)$$

2) Friction Forces and Contact Load

Asperity contact model of Greenwood and Tripp [ii] was used to calculate the contact load that is

$$p_c = KE'F_{2.5}(H_\sigma) \quad (4)$$

Where;

$$K=\frac{16\sqrt{2}}{15}\pi\left(N\beta'\sigma\right)\sqrt{\frac{\sigma}{\beta'}}$$

and

$$E'=\frac{1}{\dfrac{1-\upsilon_1^2}{E_1}+\dfrac{1-\upsilon_2^2}{E_2}}$$

β'= Asperity radius of curvature.
N= Number of asperities per unit contact area

$F_{2.5}(H_\sigma)$ = probability distribution of asperity heights.

Formula by [xxiii] for surface roughness having Gaussian distributed asperities as follows:

$$F_{2.5}\left(H_\sigma\right)=\begin{Bmatrix}A\left(\Omega-H_\sigma\right)^Z\\0\end{Bmatrix} \quad (5)$$

And
$A = 4.4068\text{x}10^{-5}$, $\Omega = 4.0$ and $Z = 6.804$, K as $1.198\text{x}10^{-4}$ by [xxiii]

In mixed lubrication solid-to-solid contact is also contributed to the skirt friction. For this purpose by using dry friction coefficient surfaces contact friction pressure can be determined. So, the friction force on the skirt surface is calculated by the following equation.

$$F_f=-sign(U)\int_A\left\{\frac{\mu|U|}{h}\left[2V_{r1}\right]+\mu_f p_c\right\}dA \quad (6)$$

III. Methodology

Lateral motion of the piston of heavy duty diesel engine was analyzed by the MATLAB code. Hydrodynamic film thickness and hydrodynamic pressure were solved iteratively in MATLAB.

A. Assumptions & Simplifications

1) Thermal and Elastic Deformations

Temperature variations in the piston cylinder and skirt were neglected. Temperature varies with respect to time at the top level of piston, at the upper portion of compression ring and between the two compression rings, but the upper part of the piston is relatively away from the skirt of the piston so temperature remains constant at the surface of piston skirt. Temperature didn't change for the whole 720 CA at stable speed and load. However cylinder bore and piston skirt elastic deformation vary with time due to the change in hydrodynamic pressure in cylinder bore and piston skirt interaction in result of that hydrodynamic film thickness varies. Sometimes film thickness reaches the value of nominal clearance. However, determination of the elastic deformation is necessary to form the comprehensive sub-model of the piston secondary motion.

2) Supply of Oil

Inlet conditions ensuring partially flooded lubrication is applied in the process. At the start of the process there is no secondary motion due to which hydrodynamic film thickness is maximum at the start of the process at 0° of CA that is h_{max}. This film thickness value varies as the CA increases to its maximum value by generating secondary motion.

3) Fluid & Flow Properties

Newtonian and incompressible fluid was used as the lubricant in the piston cylinder assembly. Hydrodynamic pressure does not changes the viscosity of the oil instead it changes with the change of temperature. Since temperature is considered as constant so viscosity of the fluid does not change at all throughout the process. As viscosity changes with respect to temperature so, two different viscosities at two different average contact temperature are available as:

$T_{constant} = 24°c \qquad \mu = 0.134 Pa.s$

$T_{constant} = 70°c \qquad \mu = 0.023 Pa.s$

The flow is considered as steady state.

4) Surface properties

Rough surfaces containing asperities comparatively selected by the Gaussian distribution were taken for both skirt of the piston and cylinder. Nonetheless the processes of coating, laser surface texturing and honing which apply macroscale texturing were not considered in this process.

5) Geometrical and Structural Simplifications

In this study the moments and forces which were acting on the piston skirt and the lubrication of the piston skirt were inculcated. The piston rings' effects such as addition in the friction of the piston and restricting the secondary motion of the piston and secondly the ring determines thickness of inlet oil supply throughout piston's motion towards top dead center and affects the skirt of the piston, were not considered into account. The surface of the skirt was considered as purely cylindrical. With current shape of the skirt model is effective for the small reciprocating compressors containing oil-lubricated pistons which are usually used in domestic refrigeration units.

B. Hydrodynamic Pressure Distribution by solution of Reynolds equation

Distribution of pressure between coarse surfaces is controlled by Reynolds equation which is modified by using different techniques. In the case of this model, in which one surface is stationery and one is moving Reynolds equation will be solved by using finite differencing scheme. Discretization is carried out to convert Reynolds equation from its differential form to the discrete form and then by using the following parameters Reynold equation is non-dimensional as Thus modified Reynold equation will be of the form

$$\frac{\partial}{\partial X}\left(H^3\frac{\partial P}{\partial X}\right)+\frac{\partial}{\partial Y}\left(H^3\frac{\partial P}{\partial Y}\right)=U^*\left(\frac{\partial H}{\partial X}+\sigma^*\right)+\beta\frac{\partial H}{\partial T} \quad (7)$$

Where; $X=\frac{2x}{L}$, $Y=\frac{2y}{L}$, $H=\frac{h}{c}$, $T=t\omega$,

$U^*=\frac{U}{r\omega}$, $P=p\frac{c^2}{3\mu r\omega L}$, $\sigma^*=\frac{\sigma}{c}$

And $\beta=\frac{L}{r}$ is squeeze film factor.

Now finite differencing substitutions are acquainted in the equation (7). For any given property, Ψ discretization can be carried out in X and Y-directions as given in equations (8-11), using the representations shown in Fig. 4-1 where S, E, N and W stand for, correspondingly, south, east, north and west adjacent nodes of node *P*.

$$\frac{\partial\psi}{\partial X}=\frac{\psi_{i+1,j}-\psi_{i-1,j}}{2\Delta X} \quad (8)$$

$$\frac{\partial\psi}{\partial Y}=\frac{\psi_{i,j+1}-\psi_{i,j-1}}{2\Delta Y} \quad (9)$$

$$\frac{\partial^2\psi}{\partial X^2}=\frac{\psi_{i+1,j}-2\psi_{i,j}+\psi_{i-1,j}}{(\Delta X)^2} \quad (10)$$

$$\frac{\partial^2\psi}{\partial Y^2}=\frac{\psi_{i,j+1}-2\psi_{i,j}+\psi_{i,j-1}}{(\Delta Y)^2} \quad (11)$$

$$3H^2\frac{\partial H}{\partial X}\left(\frac{\partial P}{\partial X}\right)+H^3\frac{\partial^2 P}{\partial X^2}+3H^2\frac{\partial H}{\partial Y}\left(\frac{\partial P}{\partial Y}\right)+H^3\frac{\partial^2 P}{\partial Y^2}=U^*\left(\frac{\partial H}{\partial X}+\sigma^*\right)+\beta\frac{\partial H}{\partial T} \quad (12)$$

Now by discretizing the equation (13)

$$\left(DC*DE\right)+H^3DE+(DF*DG)+H^3DH=U^*\left(DC+\sigma^*\right)+\beta\frac{\left(H_{i,j}\right)^t-\left(H_{i,j}\right)^{(t-\Delta t)}}{\Delta T} \quad (13)$$

Where;

$$DC=3H^2\frac{H_{i+1,j}-H_{i-1,j}}{2\Delta X}$$

$$DD=\frac{P_{i+1,j}-P_{i-1,j}}{2\Delta X}$$

$$DE = \frac{P_{i+1,j} - 2P_{i,j} + P_{i-1,j}}{(\Delta X)^2}$$

$$DF = 3H^2 \frac{H_{i,j+1} - H_{i,j-1}}{2\Delta Y}$$

$$DG = \frac{P_{i,j+1} - P_{i,j-1}}{2\Delta Y}$$

$$DH = \frac{P_{i,j+1} - 2P_{i,j} + P_{i,j-1}}{(\Delta Y)^2}$$

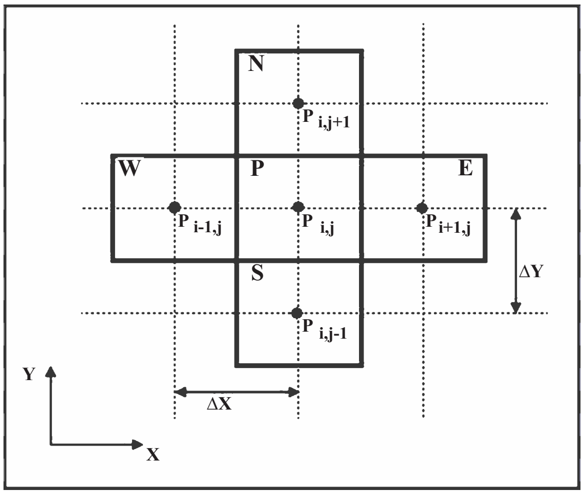

Fig. 3. Notation for the nodes

The term on the most right side of equation (12) is discretized by means of the earlier local thickness values and non-dimensional time increase and is called squeeze film velocity.

Once position of the piston is estimated hydrodynamic film thickness and squeeze film velocity can be calculated. β, ΔX, ΔY, U* and σ* from the input values. So, hydrodynamic pressure distribution can be calculated by solving equation (12) iteratively. Equation is transformed in the general form of the variables for further calculations.

$$AW_{i,j}P_{i-1,j} + AE_{i,j}P_{i+1,j} + AS_{i,j}P_{i,j-1} + AN_{i,j}P_{i,j+1} + AP_{i,j}P_{i,j} = S_{i,j} \qquad (14)$$

Where

$$AW_{i,j} = \left(\frac{H_{i,j}}{\Delta X}\right)^2 * \left[H_{i,j} - 0.5*\left(H_{i+1,j} - H_{i-1,j}\right)\right]$$

$$AE_{i,j} = \left(\frac{H_{i,j}}{\Delta X}\right)^2 * \left[H_{i,j} - 0.5*\left(H_{i+1,j} - H_{i-1,j}\right)\right]$$

$$AS_{i,j} = \left(\frac{H_{i,j}}{\Delta Y}\right)^2 * \left[H_{i,j} - 0.5*\left(H_{i,j+1} - H_{i,j-1}\right)\right]$$

$$AN_{i,j} = \left(\frac{H_{i,j}}{\Delta Y}\right)^2 * \left[H_{i,j} + 0.5*\left(H_{i,j+1} - H_{i,j-1}\right)\right]$$

$$AP_{i,j} = -2\left(H_{i,j}\right)^3 * \left[\frac{1}{\Delta X^2} + \frac{1}{\Delta Y^2}\right]$$

$$S_{i,j} = \frac{U^*}{2\Delta X}\left(H_{i+1,j} - H_{i-1,j}\right) + \beta \frac{\left(H_{i,j}\right)^t - \left(H_{i,j}\right)^{(t-\Delta t)}}{\Delta T}$$

On the surface of the skirt mesh is generated containing equidistance nodes for the solution of the general equation. Considering zero movement of the piston in pin axis. For the lateral motion of the piston, symmetric plane at right angles to the pin axis is defined.

Due to the secondary motion of the piston skirt, lubrication is not same everywhere at the piston skirt. A meshed skirt of piston is shown in Fig. 4-3. Angle of lubrication across the skirt surface is θ_{lub}. Though, Compressors use cylindrical ring less pistons. As the skirt is symmetric so its half surface was taken for the simplicity of the calculations. Half surface of skirt then converted to the straight line by the relation of

$x = z$

$y = r\theta$

Mesh can be formed by simply describing the nodes at the surface of the skirt. This mesh is given in figure A.1. In this mesh some nodes are outside the lubricated region to which pressure was set as crankcase pressure and remaining nodes are within the lubricated region to which iterations were carried out. Modified mesh is given in Fig. A. 2. Coordinates of the mesh were donated with i and j in a way

i=1, 2, 3,……………,m-1, m

j=1, 2, 3,……………,n-1, n

At x=0 and at x=L the pressure values are set as P1 and P2 respectively which will be treated as trailing and leading edge liable on the direction of instant motion of the piston. As there is no flow on the nodes present on the symmetry line so the pressure gradient will be zero in y direction. Neighboring nodes have same pressure. For a mesh of (i x j) these conditions can be written in non-dimensional form as:

At x=0, $P_{1,j} = P1$ (15)

Atx=2 $P_{m,j} = P_2$ (16)

For Y=0, $\frac{\partial P}{\partial Y} = 0$ thus $P_{i,2n-2} = P_{i,2}$ (17)

For $Y = 2\pi \frac{r}{L}$ $\frac{\partial P}{\partial Y} = 0$ thus $P_{i,n+1} = P_{i,n-1}$ (18)

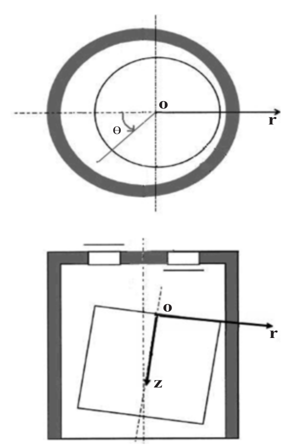

Fig. 4. Cylindrical coordinates moving with the piston

For the domain in solution of the internal combustion engine piston in addition to these conditions few more conditions are also used.

For $Y = 2\theta_{\text{lub}} \dfrac{r}{L} \qquad P_{i,n_{\text{lub}}} = P_2$ (19)

For $Y = 2\left(\pi - \theta_{\text{lub}}\right)\dfrac{r}{L} \qquad P_{i,(n-n_{\text{lub}}+1)} = P_2$ (20)

For $2\theta_{\text{lub}} \dfrac{r}{L} < Y < 2\left(\pi - \theta_{\text{lub}}\right)\dfrac{r}{L}$

$$P_{i,n_{un\,\text{lub}}} = P_2 \tag{21}$$

$$n_{unlun} = n_{lub}+1, n_{lub}+2, ..., n-n_{lub}-1, n-n_{lub} \tag{22}$$

Boundary of the lubricated area of the skirt is defined by the node n_{lub} that is the node corresponding to the θ_{lub}. In MATLAB script this can be written as

$$n_{\text{lub}} = floor\left(\theta_{\text{lub}} \frac{n-1}{\pi}\right) + 1$$

Gauss-seidel iterations are used to calculate the hydrodynamic pressure distribution. If at each node of the mesh local convergence is satisfied then overall convergence is achieved.

C. Calculation of Hydrodynamic Film Thickness

As piston skirt and cylinder bodies are assumed as rigid, it is easier to calculate the hydrodynamic film thickness around piston skirt in cylinder of the piston. Film thickness is calculated in the model by using predicted eccentricities of the piston skirt. At each node of the mesh across the surface of the skirt, film thickness is calculated as

$$h_{i,j} = c + \left(e_t - \left(e_t - e_b\right)\frac{z_{i,j}}{L}\right) * \cos\left(\theta_{i,j}\right) + \Delta h_{i,j} \tag{23}$$

$\Delta h_{i,j}$ is the deviation of skirt from its nominal radius. In this model piston skirt is considered as symmetric so its value is taken as 1.

D. Forces and Moments Calculations

By the help of combustion chamber pressure that is created by burning of fuel gas force was calculated.

$$F_g = \pi r^2 p_g \tag{24}$$

Friction force on piston skirt was calculated using the discretized form of equation (24) as:

$$F_f = -sign(U)\, 2\sum f_{f_{i,j}} \tag{25}$$

Where

$$f_{f_{i,j}} = \left[\frac{\mu |U|}{h_{i,j}} + 2V_{r1} + \mu_f p_c\right]\Delta A \tag{26}$$

This can be termed as the friction force at each node of the piston skirt.

1) Normal Force

By the combined effect of asperity contact and hydrodynamic pressure normal forces were calculated as:

$$F_h = 2\sum\left[f_{h_{i,j}} \cos\left(\theta_{i,j}\right)\right] \tag{27}$$

Where

$$f_{h_{i,j}} = \left(Ph_{i,j} + p_{c_{i,j}}\right)\Delta A \tag{28}$$

This is normal force at each node of mesh and 2 is a multiplied due half of skirt surface is symmetric.

2) Moment due to Normal Force

Hydrodynamic moment caused by the normal forces is calculated as

$$M_h = 2\sum\left[f_{h_{i,j}} \cos\left(\theta_{i,j}\right)\left(z_p - z_{i,j}\right)\right] \tag{29}$$

1) Moment Due to Friction Force

Frictional moment was calculated as

$$M_f = 2\sum\left[f_{f_{i,j}} \cos\left(\theta_{i,j}\right)\right] \tag{30}$$

IV. RESULTS AND DISCUSSIONS

A. Hydrodynamic Pressure Distribution

In following Figures effects of piston tilt causing pressure on lubrication layer can be seen. Following figures are of pressure distribution over the skirt surface for two different crank angles.

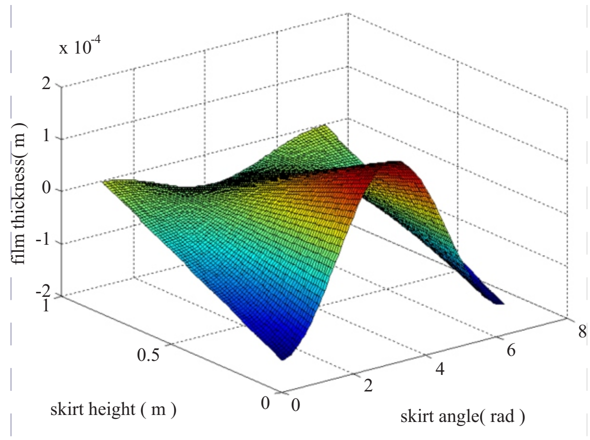

Fig. 5. Hydrodynamic Film Thickness at 90 degree CA after BDC

The above Fig. 5 shows effect on lubrication regime when the piston is moving from bottom dead center to top dead center. At this point the crank angle is 90 degrees. The results show that at anti-thrust side the film thickness is less so piston is tilted towards this side and film thickness is affected. While on the other side of piston that is on thrust side the layer is thick and was not affected.

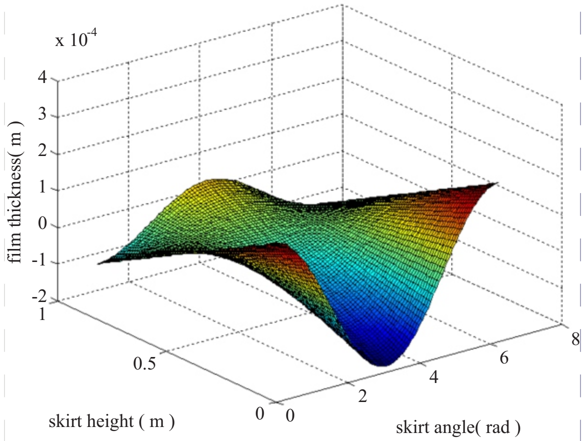

Fig. 6. Hydrodynamic Film Thickness at 90 degree CA after TDC

Fig. 6 shows the spacing between the piston skirt and cylinder liner and the film thickness profile in that spacing at 90 degree crank angle (CA) after firing the top dead center (TDC).

V. CONCLUSION

To analyze the secondary motion of the piston a mathematical model was constructed. A mixed lubrication was considered in the model. For determining the hydrodynamic fluid pressure Reynolds equation was solved iteratively by finite differencing method and the effect of surface roughness on the flow of lubricant between the piston skirt and cylinder liner was determined. To add the effect of solid contact in the hydrodynamic loading on the piston skirt and in the viscous friction, asperity contact of the two uneven surfaces was added in the model and then calculated. While the hydrodynamic lubrication and hydrodynamic pressure is determined along the skirt surface at each crank angle.

The results extracted from the research showed that hydrodynamic film thickness is maximum at the top of the skirt but as piston moves from top dead center to bottom dead center, film thickness decreases on the lower edge of the skirt and hydrodynamic pressure also acts on the skirt on thrust side of the cylinder. As piston goes upward from bottom dead center to top dead center then tilting motion of the skirt is towards the anti-thrust side of the cylinder and film thickness is maximum at the bottom of the skirt and it lowers along the surface of the skirt on the upper side and pressure development is also on anti-thrust side.

However the analysis can be further extended in future by using unconventional lubricant and additive such as low phosphorous and high molybdenum (LPHM) for better fuel economy and wear prevention,

REFERENCES

[i] M. Priest, C. M. Taylor (2000). Automobile engine tribology—*approaching the surface*. Elsevier

[ii] J. Greenwood, H. Tripp (1971). The contact of two nominal flat rough surfaces. *Instn Meth Engrs*, Tribology Group, 185, 48-51

[iii] N. Patir, H. S. Cheng (1978). An average flow model for determining effects of three-dimensional roughness on partial hydrodynamic lubrication. *Journal of lubrication Technology, 100(1), 12-17*, 100(1), 12-17.

[iv] R. Keribar, Z. Dursunkaya (1992). A comprehensive model of piston skirt lubrication (No. 920483). *SAE Technical Paper*

[v] R. Keribar, Z. Dursunkaya. (1994). A model of piston secondary motion and elastohydro-dynamic skirt lubrication. *Journal of tribology*, 116(4), 777-785.

[vi] V. Wong, T. Tian, H. Lang, Y. Sekiya (1994). A numerical model of piston secondary motion and piston slap in partially flooded elastohydro-dynamic skirt lubrication (No. 940696). *SAE Technical Paper*.

[vii] T. Kimura, K. Takahashi, S. Sugiyama (1999). Development of a piston secondary motion analysis program with elastically deformable piston skirt (No. 1999-01-3303). *SAE Technical Paper*.

[viii] I. Etsion, K. Gommed (1995). Improved design with noncylindrical profiles of gas-lubricated ringless pistons. *Journal of tribology, 117(1)*, 143-147.

[ix] A. T. Prata, J. R. Fernandes (2000). Dynamic analysis of piston secondary motion for small reciprocating compressors. *Journal of tribology, 122(4)*, 752-760.

[x] J. Yang, W. Yang, C. Wang (2001). Design of internal combustion engine piston based on skirt lubrication analysis (No. 2001-01-2486). . *SAE Technical Paper.*

[xi] B. Scholz, M. Bargende (2001). A Hydrodynamic Contact Algorithm (No. 2001-01-3596). *SAE Technical Paper*.

[xii] M. Duyar, D. Bell, M. Perchanok (2005). A comprehensive piston skirt lubrication model using a mass conserving EHL algorithm (No. 2005-01-1640). *SAE Technical Paper.*

[xiii] Y. Chung, H. J. Schock, L. J. Brombolich (1993). Fire ring wear analysis for a piston engine. *SAE Technical Paper*.

[xiv] J. E. Yun, Y. Chung, S. M. Chun, K. Y. Lee (1995). An application of simplified average Reynolds equation for mixed lubrication analysis of piston ring assembly in an internal combustion engine (No. 952562). *SAE Technical Paper*.

[xv] B. Yu, J. T. Sawicki, V. Dunaevsky (1999). Analytical solution of piston ring pack lubrication for truck air brake compressor (No. 1999-01-3769). *SAE Technical Paper*.

[xvi] R. Stanley, D. Taraza (1999). A simplified friction model of the piston ring assembly (No. 1999-01-0974). *SAE Technical Paper*.

[xvii] G. Akalin (2001). Piston ring-cylinder bore friction modeling in mixed lubrication regime: part I—analytical results. *Journal of tribology, 123(1)*, 211-218.

[xviii] Y. Harigaya, M. Suzuki, F. Toda, M. Takiguchi (2006). Analysis of oil film thickness and heat transfer on a piston ring of a diesel engine: effect of lubricant viscosity. *Journal of engineering for gas turbines and power*, *128*(3), 685-693.

[xix] M. K. Ali, H. Xianjun, L. Mai, C. Qingping, R. F. Turkson, C. Bicheng (2016). Improving the tribological characteristics of piston ring assembly in automotive engines using Al_2O_3 and TiO_2nanomaterials as nano-lubricant additives. *Tribology International*, *103*, 540-554.

[xx] Y. E. Ayranci, O. Akalin (2018). Continuous Lubricant Film Thickness Measurement Between Piston Ring and Cylinder Bore. *Journal of Engineering for Gas Turbines and Power*, *140*(7), 072802

[xxi] S. A. Qasim, M. A. Malik, M. A. Khan,R. A. Mufti (2012). Modeling shear heating in piston skirts EHL considering different viscosity oils in initial engine start up. *Journal of Engineering for Gas Turbines and Power*, *134*(3), 032802.

[xxii] V. W. Wong, S. C. Tung (2016). Overview of automotive engine friction and reduction trends–Effects of surface, material, and lubricant-additive technologies. *Friction*, *4*(1), 1-28.

[xxiii] Y. Hu, H. S. Cheng, T. Arai, Y. Kobayashi, S. Aoyama (1994), Numerical Simulation of Piston Ring in Mixed Lubrication—A Non-Axi-Symmetrical Analysis," *ASME J. Tribol., 116, pp. 470–478.*